Diameter control of single-walled carbon nanotubes using argon–helium mixture gases

Samir Farhat[a)]
LIMHP Université Paris 13, Avenue J. B. Clément 93430 Villetaneuse, France

Marc Lamy de La Chapelle and Annick Loiseau
LEM, ONERA, BP 72, 92322 Châtillon Cedex, France

Carl D. Scott
NASA, Lyndon B. Johnson Space Center ES3, Houston, Texas 77058

Serge Lefrant
IMN, Université de Nantes, BP 32229, 44322 Nantes Cedex 3, France

Catherine Journet
DPM, Université de Lyon I, 69622 Villeurbanne Cedex, France

Patrick Bernier
GDPC, Université de Montpellier II, 34095 Montpellier Cedex 5, France

(Received 27 February 2001; accepted 18 June 2001)

A method is reported for controlling the diameter of single-walled carbon nanotubes (SWCNTs) during the electric-arc-discharge process. Using argon as inert atmosphere provides smaller diameters as compared with those when pure helium is used. Varying the gas mixture from argon to helium changes the diameter distribution to higher values. A linear fit of the average diameter shows a 0.2 Å diam decrease per 10% increase in the argon–helium ratio. © *2001 American Institute of Physics.* [DOI: 10.1063/1.1390526]

I. INTRODUCTION

Interest in single-walled carbon nanotubes (SWCNTs) has been stimulated by the properties and potential applications of these novel one-dimensional objects.[1] This interest has generated many experimental and theoretical studies to provide an understanding of the growth mechanism. These studies investigate how parameters of the process influence purity, tube length and diameter, degree of helicity, intertube spacing, packing density, alignment, etc. Several laboratory-scale methods have been proposed to produce SWCNTs including condensation of arc[2,3] and laser[4,5] vaporized carbon in the presence of catalysts, decomposition of hydrocarbons on supported[6–9] or entrained[10–13] catalysts, and the decomposition of carbon monoxide on supported catalysts.[6,14] More recently, Smalley's group[15,16] proposed a new technique involving high pressure decomposition of CO on gas phase metallo-organic $Fe(CO)_5$. For the future, there is an important challenge for scaling up, optimizing and controlling this process to make it commercially viable. This could be achieved by studying growth conditions, such as temperature, pressure, and kinetics. From this understanding more efficient synthesis techniques may be developed and may yield very narrow property distributions and high production rates. Nanotube diameter is an important parameter to be controlled; and successful preliminary results have been obtained. Smalley and co-workers[5] show that the SWCNTs produced by their laser/oven method are nearly uniform in diameter (1.38 nm) and self-organized into ropelike crystallites consisting of up to a few hundreds of SWCNTs in a two-dimensional triangular lattice. Robertson *et al.*[17] and Lucas *et al.*[18] studied the stability of nanotubes as a function of their diameter using classical mechanics calculations. They pointed out that larger diameter tubes are more stable than smaller ones. Kiang *et al.*[19] analyzed diameter distributions data from the literature for nanotubes produced by different methods. They conclude that the main peak in the distribution occurs at 1–2 nm when transition metals, Fe or Co, are used as catalyst. They explain the observed narrow diameter distribution and the occurrence of only single-wall tubes (very small number of double-wall tubes over thousands tubes observed) by the inhibition of nucleation of additional layers and the importance of growth kinetics rather than energetic considerations in the nanotube formation process. By adding elements such S, Pb or Bi as co-catalysts to cobalt, the main peak in the distribution occurs at 1–2 nm. The yield of nanotubes is improved but the diameter of some tubes is greatly increased to 3–6 nm. Nikolaev *et al.*,[20] reported that starting with SWCNTs with a diameter of 1.36 nm and annealing them under a flowing hydrogen atmosphere at 1500 °C it is possible to double the diameter of 60% of SWCNTs to 2.7 nm. Occasionally, the diameter of some tubes has tripled to 4.1 nm. To explain this result, they proposed a coalescence mechanism in which H-atoms attack the side of one nanotube, producing a defect which propagates to an adjacent tube, leading to a larger diameter and a more thermodynamically stable tube. These investigations are of

[a)]Author to whom correspondence should be addressed. Tel: 33 1 49 40 34 18; fax: 33 1 49 40 34 14; electronic mail: farhat@limhp.univ-paris13.fr

primary importance in several potential applications, such as hydrogen storage.[21–25] It was found using Monte Carlo simulations[24,25] that the amount of reversible hydrogen adsorbed in the bundles of SWCNTs depends on tube diameter and intertube spacing. In addition, it has been demonstrated through theoretical predictions of Hamada *et al.*,[26] and Saito *et al.*[27,28] that the electronic properties of individual nanotubes can strongly vary with tube diameter and chirality. Nanotubes are metallic or semiconducting depending on the *n* and *m* integers defining the chiral vector. A similar strong modification arises for the magnetic properties of SWCNTs which exhibit a paramagnetic to diamagnetic transition when the nanotube radius increases above a critical radius of 0.64 nm (Davids *et al.*[29]). Finally nanotubes with a large enough internal diameter may have interesting applications as x-ray or thermal neutron wave guides.[30] So, in order to control the final properties, and hence applications, nanotube diameter control is of great importance. Depending on the process used to produce SWCNTs, several macroscopic parameters can affect tube diameter such as the nature of inert gas, the pressure, the kind of catalyst, the power density, and the geometry of the reactor. The nature of inert gas appears to be a sensitive parameter to control nanotube diameter; and this is probably due to its influence on heat transfer and diffusion in the reactor. Several researchers have noted the importance of thermal conditions on nanotubes growth in the arc[31,32] and laser processes.[33] For the existing laboratory-scale reactors, temperature control is achieved by adjusting the power in the arc and laser processes and/or by adjusting the water cooling flow rate in the arc method; or finally by maintaining a constant temperature using an oven in the laser process. As a new control feature, a mixture of argon and helium is used in this work as the inert gas for the arc process. The thermal conductivity of argon is about eight times smaller than helium. Varying the argon–helium gas ratio alters the heat transfer between the anode and the cathode. This provides a useful insight into basic parameters which affect nanotube growth and provides a viable method to control nanotube diameter during the electric-arc-discharge method.

II. EXPERIMENTS

The standard arc-evaporation method as developed by Bernier and co-workers[3] were used in this study to produce nanotubes. The reactor consists of a water-cooled reaction chamber with two cooled graphite rods. For the anode, a 3 mm diam hole 100 mm long was drilled in a pure graphite 6 mm diam rod of 150 mm long. It was filled with a mixture of graphite, nickel, and yttrium powders with diameter of few micrometers. The final molar ratio of C/Ni/Y including the outer graphite shell was 94.8 : 4.2 : 1. The cathode is made of pure graphite. The distance between the anode and the cathode was maintained at about 3 mm by moving the anode toward the cathode. A direct current of 100 A passes through the electrodes; and a plasma is created in the interelectrode region. Efficient operation is assumed to exist when the discharge is stable and the anode erosion rate is constant. This could be achieved by maintaining a constant voltage between the electrodes, which is closely related to the stabilization of the electrode spacing. In our system, a magnified image of the electrodes is projected onto a screen using a lens and the gap between the electrodes is controlled manually. The plasma is first ignited by contact between the anode and the cathode, which elevates the temperature of the contact point until evaporation of the anode material. Then, the anode is moved back to maintain a desired gap between the growing deposit on the cathode and the burning anode. An active plasma zone bounded by the deposit and the anode is created. The function of this zone is to produce optimally carbon and catalyst vapors, which then diffuse to the cooled reactor regions. Carbon species deposit to form a collaret around the cathode deposit and soot is deposited on the reactor walls. The high temperature near the anode and the high energy densities in the plasma insure total vaporization of the anode material. The water cooled cathode leads to a high quench rates and high levels of supercooled or supersaturated vapor with nanotube formation. The quench process is uncontrolled, but we usually obtain various products; soot on the reactor walls, weblike structures between the cathode and the chamber walls, a deposit at the cathode's end, and a rubberlike collaret around this deposit. We focused this study only on the collaret, which is known to contain the highest density of SWCNTs.[34] A typical TEM micrograph of this collaret is shown in Fig. 1. From TEM observations it is believed that at a gross level, vapor from the plasma precipitates to form small catalyst particles in the nanoscale range from which nanotubes nucleate and grow

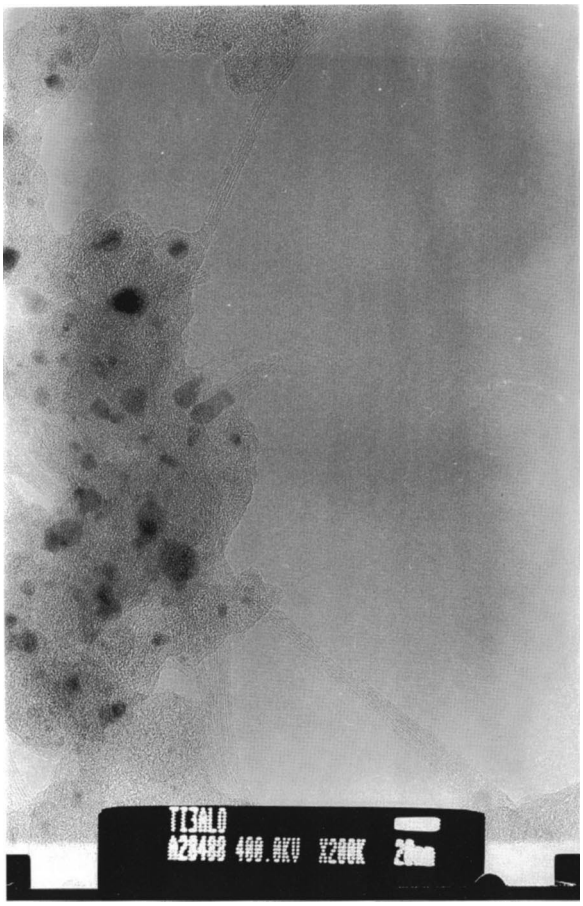

FIG. 1. TEM image of the collaret obtained with pure He at pressure of 660 mbar.

rapidly in the region of high carbon density. These nanotubes are always capped, and are never found to have any metal particles at their ends. They seem to grow either in bundles or as individual tubes that coalesce readily into bundles.

The procedure of nanotube production consists of evacuating the reactor and then filling it with the buffer gas mixture at the desired pressure. This is followed by the anode burn, product collection, and analysis. Because optimum nanotube yield was found at a pressure of 660 mbar for pure helium, and at a pressure of 100 mbar for pure argon,[34] the total pressure of the mixture was varied arbitrarily between 100 mbar and 660 mbar using a linear fit given in Table I. We characterized the collaret obtained under these various experimental conditions by Raman spectroscopy using a Jobin Yvon T64000 spectrophotometer. Spectra have been recorded at room temperature in ambient air with an argon laser at 514.5 nm. The use of a microprobe has allowed us to focus the laser spot on the micrometer scale. Spatially resolved features can be obtained providing clear indications of the distribution of in the samples.

Indeed, two main regions can be distinguished in a Raman spectrum as actually relevant to SWCNTs: (1) the high frequency (1500–1600 cm^{-1}) and 2) the low frequency (100–250 cm^{-1}) ranges. The first range gives evidence of the existence of the SWCNTs in the sample.[35,36] In this region, the most intense band of the spectrum can be seen at 1590 cm^{-1} with at least three components at 1530, 1550, and 1565 cm^{-1} with decreasing relative intensities. This band profile has been assigned to the splitting of the E_{2g2} graphite mode, due to the curvature of the graphene sheet. Since the other graphitic materials do not show as many bands in this region, the observation of these bands can be considered as a signature of the presence of SWCNTs in the sample. In the second region, we can also observe several peaks located between 148 and 200 cm^{-1}. Their relative intensities change with the position of the laser spot on the sample[36] and with the excitation wavelength. These bands are assigned to one of the A_{1g} radial breathing modes of the SWCNTs.[37,38] The frequency ν of this mode depends directly on the nanotube diameter d by the correlation $\nu\,(\mathrm{cm}^{-1}) = 2237.5/d\,(\text{Å})$.[33] Thus, to each peak, we can assign one specific diameter. It is known that the lower the frequency, the larger the diameter. The positions of these peaks yields some information on the diameters of the nanotubes in the laser spot. Moreover, for a given laser wavelength, the relative intensity of each peak corresponds to the proportion of each specific diameter that is resonantly excited. If on the same laser spot, we change the wavelength used, we can observe different size tubes that are excited. We associate these differences to resonance effects. Indeed, it has been demonstrated the existence of singularities in the electronic density of states in the SWCNTs. The position of these singularities depend both on the diameter and on the semiconducting or metallic tube behavior. By changing the excitation energy, we are able to excite electronic transitions that corresponds to specific tube diameters and/or metallic or semiconducting behavior. To avoid this resonance effect and the related change of the relative intensities in the breathing mode, we used only one excitation wavelength: 514.5 nm from an argon ion laser. We then assume that the recorded intensity evolution is only due to the diameter distribution. Therefore, the group of peaks gives an indication of the diameter distribution at the laser spot at several locations on the sample. It should be noted that with this wavelength we observe preferentially the semiconducting tubes. This does not mean that the metallic tubes do not contribute to the Raman intensity. In our work, all tube diameters have been estimated from the formula given by Bando *et al.*;[33] $\nu\,(\mathrm{cm}^{-1}) = \alpha/d$ with $\alpha = 2237.5\ \mathrm{cm}^{-1}$ Å. Recently, Jorio *et al.*[39] have given a new value for α which should be equal to 248 cm^{-1} nm. The effect of the difference between these two values is only to shift the tube diameters, living them in the same relative positions. The choice of α does not alter the conclusions of the study.

III. RESULTS AND DISCUSSION

Results are given of Raman spectra of nanotubes produced in pure helium, pure argon and in mixtures of these gases.

A. Pure helium

For pure helium, various pressures ranging from 100 to 1200 mbar have been tested. The macroscopic products obtained are different depending on the pressure.

(1) At low pressures ranging from 100 to 300 mbar, a small hard gray deposit 1 g weight and 1.5 cm long grows from the surface of the cathode. Around this deposit is formed a small black and crumbly collaret of about 200 mg weight. Crumbly soot is also collected from the reactor walls.
(2) At increased helium pressure between 400 and 800 mbar, we observe a very long deposit (2.5 g, 5.5 cm long) at the surface of the cathode and a very large and spongy black collaret (600 mg) with a soft belt around it. A lot of weblike structures can be found growing from the cathode to the reactor walls where rubbery soot is now collected in large pieces.
(3) At higher pressures ranging from 900 to 1200 mbar, a medium (2 g, 3.5 cm long) deposit is grown on the cathode and the collaret is very small (20 mg). A few webs are found and the soot on the reactor walls is again crumbly.

We have found that the largest amount of collaret is obtained at a pressure around 660 mbar. Raman spectra given in Fig. 2 show that whatever the pressure used, we always observe radial breathing mode peaks with the same positions in the 100–250 cm^{-1} range. Occasionally, we see changes in the relative intensity distributions of these peaks at various places of the collaret due to its inhomogeneity. We have never observed a predominance of one peak which could signify that one particular diameter is favored at a given particular pressure. So whatever the pressure used, the diameters of the nanotubes are always similar, going from 11 to 15 Å. The only change observed is the number of areas of the sample containing SWCNTs. Indeed, as the use of a microprobe allows us spatial resolution of 1 μm^2, we can easily distinguish the areas with SWCNTs and those without. The

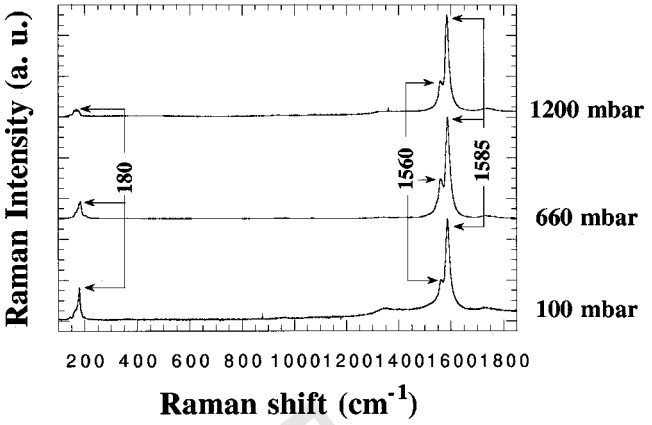

FIG. 2. Raman spectra of collaret obtained with pure He at pressure ranging from 100 to 1200 mbar at a laser energy of 2.41 eV.

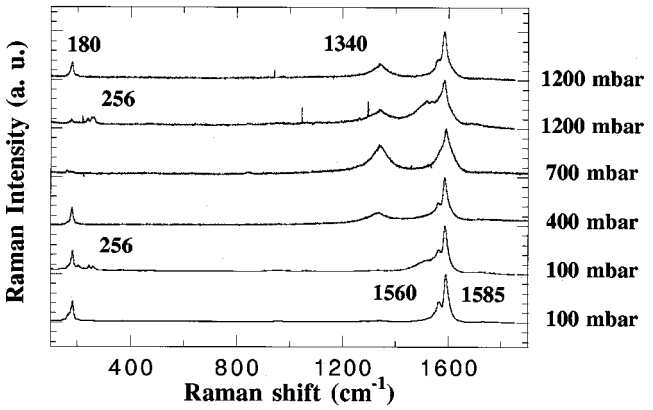

FIG. 3. Raman spectra of collaret obtained with pure Ar at pressure ranging from 100 to 1200 mbar at a laser energy of 2.41 eV.

number of areas containing SWCNTs decreases for pressures other than 660 mbar. As a consequence, the quantity of SWCNTs produced is less for pressures different from 660 mbar. We conclude that the pressure only has an influence on the rate of the production, with the existence of an optimum pressure, whereas it has no influence on the structure of the nanotubes.

B. Pure argon

A similar pressure dependence is also found when using pure argon instead of helium.

(1) We find that at low pressures ranging from 100 to 300 mbar, a medium deposit of 2 g weight and 3 cm long, a very small collaret 50 mg, no webs, and a small amount of crumbly soot.
(2) At intermediate pressures ranging from 400 to 800 mbar, the deposit is bigger (3 g, 6 cm long) but the collaret is always small (20 mg) and no webs are formed. A very small quantity of crumbly soot is collected from the reactor walls.
(3) Between 900 and 1500 mbar, the deposit is quite long (3 g, 5 cm long), the collaret is smaller (10 mg), the soot is crumbly and no webs are observed. The collaret mass is maximum for a pressure around 100 mbar.

With Raman spectra given in Fig. 3, we can make similar observations as with helium; the nanotube diameter distribution is independent of pressure, and there is an optimum pressure where the Raman signal is strongest.

In comparing the two gases, two differences can be seen. First, the optimum pressure is near 100 mbar for argon vs 660 mbar for helium. Second, for pure argon, Raman peaks are found between 200 and 260 cm^{-1} which could be associated with nanotubes with diameters between 0.8 and 1.1 nm. These peaks are not seen when helium is present. Thus, it seems that with argon, we form nanotubes with diameters from 1.2 to 1.4 nm, and as small as about 0.9 nm. We never observe such small diameters with helium. Finally, we can affirm that for a single gas (helium or argon), there is no influence of the pressure on the structure of the nanotubes but only on their relative density.

C. Helium–argon mixtures

Raman experiments have also been performed at each condition in Table I. We have recorded spectra obtained from at least ten different points to get an overall view of each sample. Typical SEM pictures for collaret produced using argon, helium and their mixture as inert gas are shown in Fig. 4, and a representative spectrum from these samples is shown in Fig. 5. From the SEM images, we can see that the density of nanotubes decreases with argon mole fraction. In Fig. 6, the low frequency range has been scaled up to better observe the breathing modes. We can clearly see an evolution of the relative intensities of the whole group of bands assigned to the breathing mode. Indeed, from 0 to 100% of argon, the lower frequency bands (135, 145, and 160 cm^{-1}) decrease in intensity, whereas the higher frequency ones (170 and 180 cm^{-1}) grow. In all spectra, we observe bands at 145, 160, 170, and 180 cm^{-1}. The relative intensity of these bands changes drastically as the atmosphere varies from pure helium to pure argon. For example, at 20% argon, the band with highest intensity is at 160 cm^{-1}, whereas at 100% argon, the most intense is the 180 cm^{-1}. Moreover, some specific bands appeared in specific conditions. At 20% argon, a peak at 135 cm^{-1}, which corresponds to a tube diameter near 1.65 nm, is visible which confirms that an inert atmosphere containing a little argon favors the formation of large tube diameters. On the other hand, for 100% argon, we can observe the appearance of some bands at a frequency higher than 200 cm^{-1} which corresponds to tubes with diameters smaller than 1.1 nm, as also seen in experiments with pressure variation.

TABLE I. Total and partial pressures vs argon molar percentage in the chamber.

Experiment	%Ar	P_{He} (mbar)	P_{Ar} (mbar)	P_{tot} (mbar)
1	0	660	0	660
2	20	440	110	550
3	40	261	174	435
4	60	130	195	325
5	80	40	170	210
6	100	0	100	100

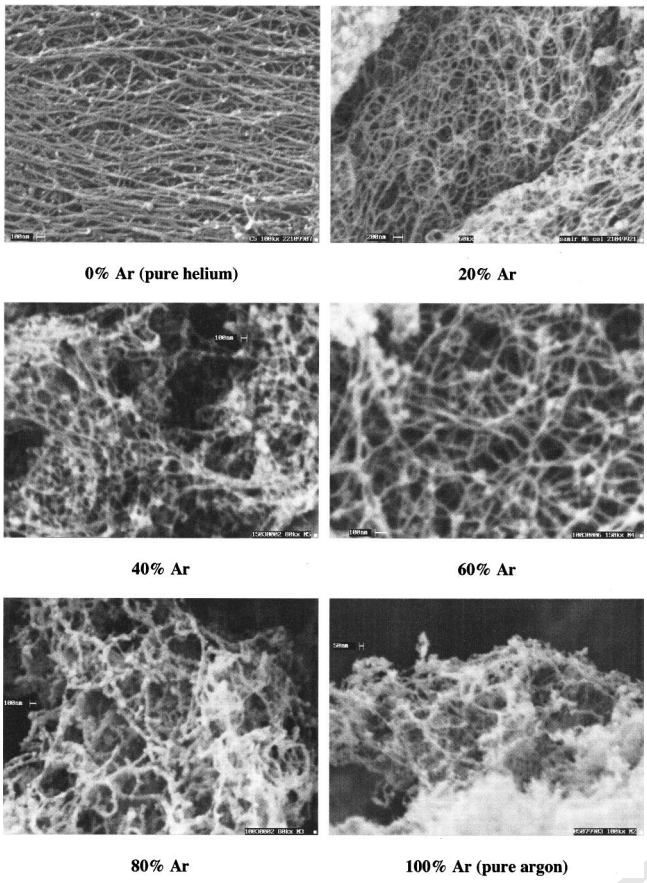

FIG. 4. SEM images of collaret obtained with different argon–helium mixture.

To determine the diameter distribution, we have fitted several Lorentzian shapes (one shape per band) to the whole group of peaks assigned to the breathing mode. In this way, we have been able to get the proportion of each diameter for all recorded spectra. We can then calculate an average diameter distribution and an average diameter from all areas of the same sample. Of course not all diameters are excited by a single laser frequency; therefore the sample is biased toward those peaks that are observable with argon ion laser. We assume that the diameter distribution and average diameter depend on the inert atmosphere. This dependence is

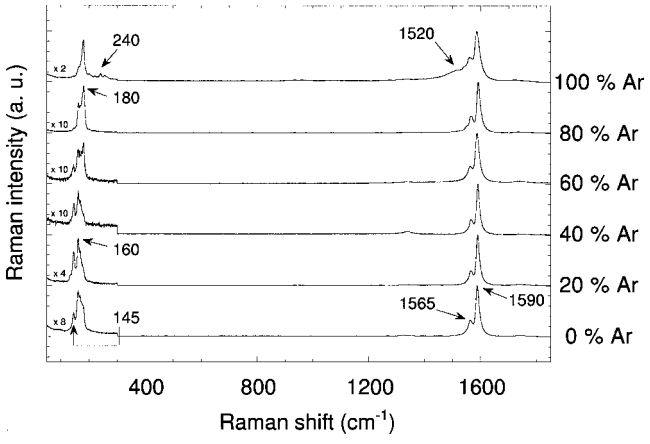

FIG. 5. Raman spectra for a mixture of Ar/He at a laser energy of 2.41 eV.

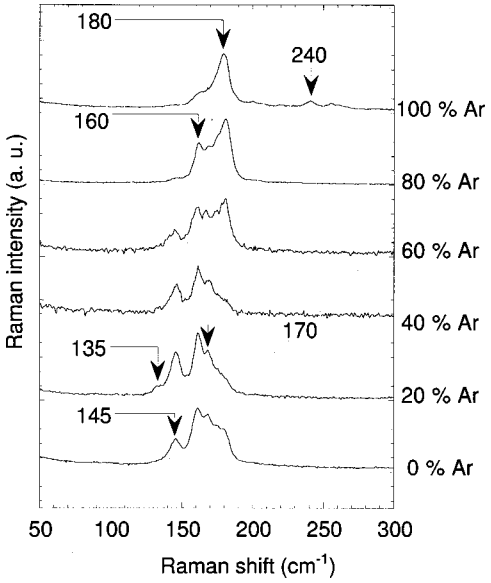

FIG. 6. Low frequency range magnification of Fig. 5 showing the breathing modes.

given in the histograms of Fig. 7 and on the curve of Fig. 8. First, we have noticed that all samples produced with an inert atmosphere containing argon are spatially very homogeneous with little difference from one region to another. In the case of 100% helium, we get very inhomogeneous sample as it has been reported elsewhere.[3] This can be explained by the amount of collaret produced with these various atmospheres. Indeed, when pure helium is used in the chamber, the mass of product is much larger than with argon. So, with helium, more nanotubes are produced than with argon. This implies that the local conditions, and notably the temperature, are less homogeneous with helium than with argon since the radius of collaret is much larger. Also the tube diameters produced are less homogeneous. The introduction of some argon shifts the diameter distribution toward smaller diameters, and the average tube diameter decreases linearly as function of the percentage of argon, going from near 1.4 nm to near 1.2 nm.

This means that carbon condensation in the arc is effected by the way that the vapor containing carbon species and metal atoms are cooled in the reactor chamber. This has at least two consequences on the nanotube growth.

(i) The first consequence is on the size of metal particles formed; the smaller thermal conductivity of argon leads to higher quenching rates and hence to smaller metal particles. This may indicate that tube diameter is determined by the size of the catalytic particle, as observed experimentally by Dai *et al.*[14] for SWCNTs grown by disproportionation of carbon monoxide. In fact, this result is in contradiction with the growth mechanism proposed by Smalley's group[5] which indicates that the SWCNT diameter is dictated by energetic considerations. We believe that coupling an oven to the laser process may maintain a more uniform cooling of the species from the plasma plume, and explains the nearly uniform diameter (1.38 nm) ob-

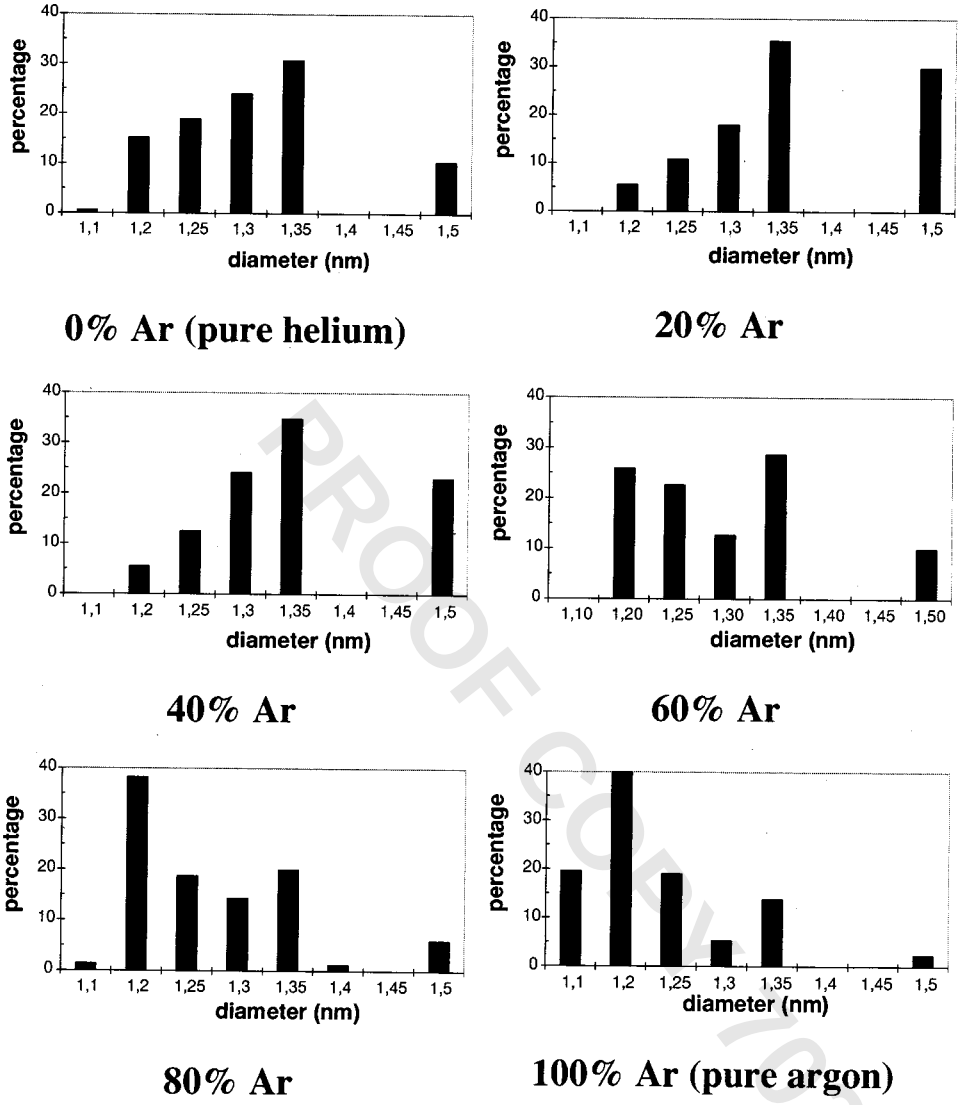

FIG. 7. Histograms showing frequency of SWCNTs at different diameter for different mixture of argon and helium.

served. More recently, Munoz *et al.*,[40] reported the synthesis of SWCNTs by laser ablation without additional heating and under atmospheres of argon, nitrogen, mixture of argon/nitrogen, and helium. They found that these different gases affect the yield of nanotubes, the amorphous carbon content, and the texture of the product. They did not report diameter distributions for these experiments, but we obtained a similar behavior in the product when mixing argon and helium in the arc process.

(ii) The second consequence of cooling is on the relative concentration of large carbon clusters C_{10} to C_{40} or larger which can act as nucleating species, as suggested in Ref. 41 and hence determines the diameter of the tubes. Indeed quantitative analysis of these relative concentrations needs a full multidimensional species, and energy model which is a difficult task, since fullerene chemistry is not yet fully understood.[42]

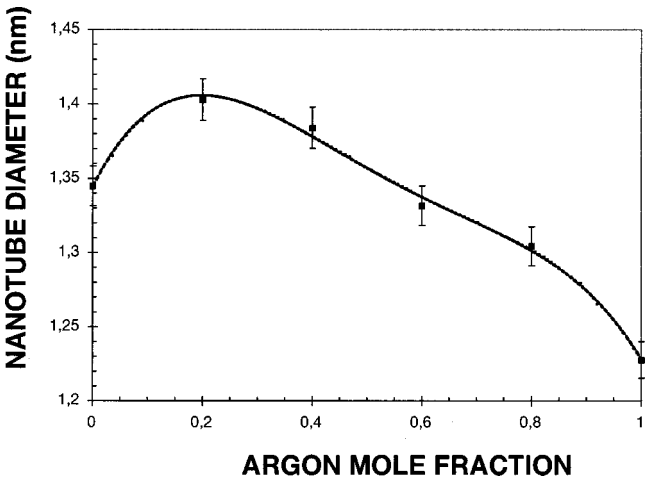

FIG. 8. Variation of the average diameter with argon mole fraction in the chamber.

IV. GROWTH MECHANISM

According to our experimental results we can propose the following scenario for nanotube formation in the arc process. The high temperature in the plasma allows total vaporization of the carbon and metal species. Somewhere between the anode and the cathode the density of C_2 particles and temperature reaches a maximum as measured by Shimada

et al.[43] by emission spectroscopy. From this region condensation of vapor species composed of carbon and metal atoms starts basically in three zones of the reactor and collects on the deposit, the cathode and the reactor wall. Forgetting for one moment the presence of any carbon species in the reactor, we can imagine that the quenching of metal vapor leads to a size and velocity segregation of metallic particles formed by condensation from the plasma. Larger diameter particles (but in nanometric scale because of the high quenching rate), could be concentrated in the central part of a turbulent jet leaving the anode, while smaller ones are in the external part of this jet directed to the region of the cathode not covered by the deposit. Because of their high molecular weight and low diffusion coefficient, the probability of finding metal catalyst particles outside the arc is low. Let us superpose on this picture the conventional fullerene formation in carbon arc processes. When the gas temperature decreases in the three zones discussed above, small fragment molecules of C_2 condense to C_3, C_4, etc. Larger clusters C_n are formed in form of chains and monocycles until C_{20}, cycle and polycycles between $n=20-30$, and fullerene shells for $n>30$.[42] We can easily understand that the central zone of the arc, rich in catalytic particles with higher diameter, is more favorable to MWNTs growth. This is observed experimentally in the deposit. The smallest catalytic particles with critical upper and lower sizes diffuse to the cathode behind and around the deposit, and form SWCNTs. When the lower critical size catalyst particle (1–2 nm) is reached, heterogeneous nucleation on the surface occurs (via kinetics by incorporation of large carbon clusters or by a ''yarmulke'' like mechanism as discussed by Dai *et al.*[14]). During their diffusion these particles continue to grow by accreting atomic metal and carbon clusters from the gas phase, while SWCNTs grow from the nuclei formed at the metal surface. When the critical upper size of the catalyst particle is reached (3–10 nm) the nanotube growth is stopped and the catalyst particle is overcoated by graphitic shells and is dead. This is observed in TEM pictures at the end of the process. According to this scenario, nanotube length is determined by the ratio of mass flux to the catalyst particle of metal to carbon, while the nanotube diameter is determined by the lower critical size of the catalyst. This parameter is sensitive to the quenching rate and hence could be controlled by the thermal conductivity of the inert atmosphere between the anode and the cathode.

V. CONCLUSIONS

Raman spectroscopy measurements performed in this work demonstrate clearly that single-walled carbon nanotubes produced with mixtures of argon and helium have different diameter distributions. Since the thermal conductivity and diffusion coefficients of the argon–helium mixture are affected by the relative concentration of the two gases, we expect that control of thermal transfer and mass diffusion, and hence condensation of atomic carbon and metals between the plasma and the vicinity of the cathode can control nanotube diameter in the arc process. This result implies that single-layer tubules nucleate and grow on metal particles with different sizes depending on the quenching rate in the plasma and suggests that temperature and carbon and metal densities affect the diameter distribution of nanotubes. Control of SWCNTs diameter remains a great challenge for scientists since the dependence of nanotube diameter with various parameters of the process is not yet fully understood. For the future, additional experiments using a mixture of inert gases with higher ratio of thermal conductivity are needed to increase the controllability of the quenching rate and hence the nanotube diameter in arc and laser processes. On the other hand, developing simpler production systems than the complex arc process will be necessary to better understand the dependence of tube diameter with these critical parameters. One direction is to develop simpler alternative approaches for *in situ* production of metal particles with a narrow distribution in the 0.5–3 nm size range.

ACKNOWLEDGMENTS

This research is supported by the CNRS-LIMHP. We thank P. Portes for SEM imaging of nanotubes, S. Sauve for helping in doing experiments, and J. F. Meunier for technical support.

[1] S. Iijima, Nature (London) **354**, 56 (1991).
[2] D. S. Bethune, C. H. Kiang, M. S. DeVries, G. Gorman, R. Savoy, J. Vazquez, and R. Beyers, Nature (London) **363**, 605 (1993).
[3] C. Journet, W. K. Maser, P. Bernier, A. Loiseau, M. L. Delachapelle, S. Lefrant, P. Deniard, R. Lee, and J. E. Fischer, Nature (London) **388**, 756 (1997).
[4] T. Guo and R. E. Smalley, in *Recent Advances in the Chemistry and Physics of Fullerenes and Related Materials* (Electrochemical Society, Pennington, 1995).
[5] A. Thess, R. Lee, P. Nikolaev, H. J. Dai, P. Petit, J. Robert, C. H. Xu, T. H. Lee, S. G. Kim, A. G. Rinzler, D. T. Colbert, G. E. Scuseria, D. Tomanek, J. E. Fischer, and R. E. Smalley, Science **273**, 483 (1996).
[6] J. H. Hafner, M. J. Bronikowski, B. R. Azamian, P. Nikolaev, A. G. Rinzler, D. T. Colbert, K. A. Smith, and R. E. Smalley, Chem. Phys. Lett. **296**, 195 (1998).
[7] A. M. Cassell, J. A. Raymakers, J. Kong, and H. J. Dai, J. Phys. Chem. B **103**, 6484 (1999).
[8] A. Fonseca, K. Hernadi, P. Piedigrosso, J. F. Colomer, K. Mukhopadhyay, R. Doome, S. Lazarescu, L. P. Biro, P. Lambin, P. A. Thiry, D. Bernaerts, and J. B. Nagy, Appl. Phys. A: Mater. Sci. Process. **A67**, 11 (1998).
[9] B. C. Satishkumar, A. Govindaraj, R. Sen, and C. N. R. Rao, Chem. Phys. Lett. **293**, 47 (1998).
[10] R. Sen, A. Govindaraj, and C. N. R. Rao, Chem. Phys. Lett. **267**, 276 (1997).
[11] H. M. Cheng, F. Li, G. Su, H. Y. Pan, L. L. He, X. Sun, and M. S. Dresselhaus, Appl. Phys. Lett. **72**, 3282 (1998).
[12] H. M. Cheng, F. Li, X. Sun, S. D. M. Brown, M. A. Pimenta, A. Marucci, G. Dresselhaus, and M. S. Dresselhaus, Chem. Phys. Lett. **289**, 602 (1998).
[13] G. G. Tibbetts, D. W. Gorkiewicz, and R. L. Alig, Carbon **31**, 809 (1993).
[14] H. J. Dai, A. G. Rinzler, P. Nikolaev, A. Thess, D. T. Colbert, and R. E. Smalley, Chem. Phys. Lett. **260**, 471 (1996).
[15] P. Nikolaev, M. J. Bronikowski, R. K. Bradley, F. Rohmund, D. T. Colbert, K. A. Smith, and R. E. Smalley, Chem. Phys. Lett. **313**, 91 (1999).
[16] K. Bradley, ''Large scale production of single wall carbon nanotubes,'' Ph.D. thesis, Rice University, 2000.
[17] D. H. Robertson, D. W. Brenner, and J. W. Mintmire, Phys. Rev. B **45**, 12592 (1992).
[18] A. A. Lucas, Ph. Lambin, and R. E. Smalley, J. Phys. Chem. Solids **54**, 587 (1993).
[19] C. H. Kiang, W. A. Goddard III, R. Beyers, and D. S. Bethune, *Carbon Nanotubes*, edited by M. Endo, S. Iijima, and M. S. Dresselhaus, 1st ed. (Pergamon, Elsevier, 1996), p. 47.
[20] P. Nikolaev, A. Thess, A. G. Rinzler, D. T. Colbert, and R. E. Smalley, Chem. Phys. Lett. **266**, 422 (1997).

[21] A. C. Dillon, K. M. Jones, T. A. Bekkedahl, C. H. Kiang, D. S. Bethune, and M. J. Heben, Nature (London) **386**, 377 (1997).
[22] M. R. Pederson and J. Q. Broughton, Phys. Rev. Lett. **69**, 2689 (1992).
[23] M. S. Dresselhaus, K. A. Williams, and P. C. Eklund, MRS Bull. **24**, 45 (1999).
[24] F. Darkrim and D. Levesque, J. Chem. Phys. **109**, 4981 (1998).
[25] Q. Wang and J. K. Johnson, J. Phys. Chem. B **103**, 4809 (1999).
[26] N. Hamada, S. Sawada, and A. Oshiyama, Phys. Rev. Lett. **68**, 1579 (1992).
[27] R. Saito, M. Fujita, G. Dresselhaus, and M. S. Dresselhaus, Phys. Rev. B **46**, 1804 (1992).
[28] R. Saito, M. Fujita, G. Dresselhaus, and M. S. Dresselhaus, Appl. Phys. Lett. **60**, 2204 (1992).
[29] P. S. Davids, L. Wang, A. Saxena, and A. R. Bishop, Phys. Rev. B **48**, 17545 (1993).
[30] N. K. Zhevago and V. I. Glebov, Phys. Lett. A **250**, 360 (1998).
[31] Y. Saito, M. Okuda, M. Tomita, and T. Hayashi, Chem. Phys. Lett. **236**, 419 (1995).
[32] M. Takizawa, S. Bandow, T. Torii, and S. Iijima, Chem. Phys. Lett. **302**, 146 (1999).
[33] S. Bandow, S. Asaka, Y. Saito, A. M. Rao, L. Grigorian, E. Richter, and P. C. Eklund, Phys. Rev. Lett. **80**, 3779 (1998).
[34] C. Journet, Ph.D. thesis, ''La production de nanotubes de carbone,'' Académie de Montpellier, Université de Montpellier II, 1998.
[35] J. Holden, P. Zhou, X.-X. Bi, P. C. Eklund, S. Bandow, R. A. Jishi, K. D. Chowdhury, G. Dresselhaus, and M. S. Dresselhaus, Chem. Phys. Lett. **220**, 186 (1994).
[36] A. Kasuya, Y. Sasaki, Y. Saito, K. Tohji, and Y. Nishina, Phys. Rev. Lett. **72**, 4434 (1997).
[37] A. M. Rao, E. Richter, S. Bandow, B. Chase, P. C. Eklund, K. A. Williams, S. Fang, K. R. Subbaswamy, M. Menon, A. Thess, R. E. Smalley, G. Dresselhaus, and M. S. Dresselhaus, Science **75**, 187 (1997).
[38] M. Lamy de la Chapelle, S. Lefrant, C. Journet, W. Maser, and P. Bernier, Carbon **36**, 705 (1998).
[39] A. Jorio, R. Saito, J. H. Hafner, C. M. Lieber, M. Hunter, T. McClure, G. Dresselhaus, and M. S. Dresselhaus, Phys. Rev. Lett. **86**, 1118 (2001).
[40] E. Munoz, W. K. Maser, A. M. Benito, G. F. De la-Fuente, and M. T. Martinez, Synth. Met. **103**, 2490 (1999).
[41] C. H. Kiang and W. A. Goddard III, Phys. Rev. Lett. **76**, 2515 (1996).
[42] A. V. Krestinin and A. P. Moravskii, Chem. Phys. Rep. **18**, 515 (1999).
[43] Y. Shimada, S. Akita, S. Suzuki, and Y. Nakayama, Electron. Commun. Jpn., Part 2: Electron. **81**, 42 (1998).